Effect of pH on the Biphasic Catalytic Hydrogenation of Benzylidene Acetone Using $CpRu(PTA)_2H$

Charles A. Mebi and Brian J. Frost*

Department of Chemistry, University of Nevada, Reno, Nevada 89557

Received December 21, 2004

The hydrogenation of benzylidene acetone has been accomplished under biphasic conditions (water/diethyl ether) utilizing $CpRu(PTA)_2H$ as the catalyst under mild conditions. The results show high selectivity toward hydrogenation of the olefin in benzylidene acetone with 4-phenylbutan-2-one as the major product. The effects of pH, hydrogen pressure, and salts on the reduction are described. The presence of anions such as BF_4^- and PF_6^- significantly improve catalytic activity, while Cl^- shuts down catalysis due to the formation of the catalytically inactive $CpRu(PTA)_2Cl$. The aforementioned factors do not influence the selectivity of the reaction. Spectroscopic studies of the nature of $CpRu(PTA)_2H$ under the reaction conditions enabled the identification of mono- and dihydride intermediates, $[CpRu(PTA)(PTAH)H]^+$ and $[CpRu(PTA)_2(H)_2]^+$, respectively. The distribution of these intermediates as a function of pH and the effect on reaction rates are presented. Reaction rate is found to increase with an increase in concentration of $[CpRu(PTA)(PTAH)H]^+$, which is the presumed active catalytic species. Based on the data presented a 1,4-conjugate addition mechanism is proposed. Finally, the solid-state structures of the mono- and diprotonated complexes of $CpRu(PTA)_2Cl$, $[CpRu(PTA)(PTAH)Cl](PF_6)$, and $CpRu(PTAH)_2Cl](PF_6)_2$ are reported.

Introduction

Water-soluble organometallic catalysts are of great interest due to their utility in aqueous biphasic catalysis.[1−4] The use of biphasic catalysis has far-reaching importance in the design of green chemical processes, which allow for the use of water as a cosolvent. Water, being nonflammable, inexpensive, readily available, and nontoxic, is probably the most desirable solvent. By modifying conditions, such as pH, the activity and selectivity of the catalyst can be modulated.[3,5−7] Since 1973, enormous effort has been made toward the development of catalytic reactions in aqueous solutions and in biphasic mixtures of water with organic solvents.[8] Water-soluble phosphines have largely been responsible for making metal complexes soluble in aqueous media. A variety of water-soluble phosphine ligands have been employed utilizing solubilizing groups such as SO_3^-, NMe_3^+, OH, or COO^-.[1,2,4] Our group has been interested in the neutral, water-soluble, and air-stable phosphine 1,3,5-triaza-7-phosphaadamantane (PTA), first synthesized by Daigle[9] and introduced into aqueous organometallic catalysts by Joó, Darensbourg, and others.[10−14] Many metal complexes of PTA have been synthesized and utilized in aqueous catalysis, particularly the hydrogenation of C=C and C=O bonds useful in the synthesis of fine chemicals, pharmaceuticals, and agrochemicals.[13,15−17]

PTA

The protonation of metal hydrides has attracted a great deal of attention in recent years owing to the formation of $M(H_2)^+$ and $M(H)_2^+$ compounds intimately involved in catalysis.[18−22] Understanding the properties

* Corresponding author. Tel: +1-775-784-1993. Fax: +1-775-784-6804. E-mail: Frost@chem.unr.edu.

(1) *Aqueous-Phase Organometallic Catalysis: Concepts and Applications*, 2nd ed.; Cornils, B.; Herrmann, W. A., Eds.; Wiley-VCH: New York, 2004.
(2) *Aqueous Organometallic Chemistry and Catalysis*; Horvath, I. T.; Joó, F., Eds.; NATO ASI Series 3; High Technology; Kluwer: Dordrecht, The Netherlands, 1995.
(3) Joó, F. *Acc. Chem. Res.* **2002**, *35*, 738−745.
(4) Joó, F. *Aqueous Organometallic Catalysis;* Catalysis by Metal Complexes 23; Kluwer Academic Publishers: Boston, 2001.
(5) Joó, F.; Kovacs, J.; Benyei, A. Cs.; Katho, A. *Angew. Chem., Int. Ed.* **1998**, *37*, 969−970.
(6) Joó, F.; Kovacs, J.; Benyei, A. Cs.; Katho, A. *Catal. Today* **1998**, *42*, 441−448.
(7) Joó, F.; Kovacs, J.; Benyei, A. Cs.; Nadasdi, L.; Laurenczy, G. *Chem. Eur. J.* **2001**, *7*, 193−199.
(8) Kuntz, E. G. *CHEMTECH* **1987**, *17*, 570−575.
(9) Daigle, D. J.; Pepperman, A. B., Jr.; Vail, S. L. *J. Heterocycl. Chem.* **1974**, *11*, 407−408.
(10) Darensbourg, D. J.; Joó, F.; Kannisto, M.; Katho, A.; Reibenspies, J. H. *Organometallics* **1992**, *11*, 1990−1993.
(11) Darensbourg, D. J.; Joó, F.; Kannisto, M.; Katho, A.; Reibenspies, J. H.; Daigle, D. J. *Inorg. Chem.* **1994**, *33*, 200−208.
(12) Laurenczy, G.; Joó, F.; Nádasdi, L. *Inorg. Chem.* **2000**, *39*, 5083−5088.
(13) Darensbourg, D. J.; Decuir, T. J.; Reibenspies, J. H. In *Aqueous Organometallic Chemistry and Catalysis*; Horvath, I. T., Joó, F., Eds.; High Technology; Kluwer: Dordrecht, The Netherlands, 1995; pp 61−80.
(14) Joó, F.; Nadasdi, L.; Benyei, A. Cs.; Darensbourg, D. J. *J. Organomet. Chem.* **1996**, *512*, 45−50.
(15) Phillips, A. D.; Gonsalvi, L.; Romerosa, A.; Vizza, F.; Peruzzini, M. *Coord. Chem. Rev.* **2004**, *248*, 955−993.
(16) Darensbourg, D. J.; Stafford, N. W.; Joó, F.; Reibenspies, J. H. *J. Organomet. Chem.* **1995**, *488*, 99−108.
(17) Kovacs, J.; Todd, T. D.; Reibenspies, J. H.; Joó, F.; Darensbourg, D. J. *Organometallics* **2000**, *19*, 3963−3969.
(18) Crabtree, R. H. *Acc. Chem. Res.* **1990**, *23*, 95−105.
(19) Clapham, S. E.; Hadzovic, A.; Morris, R. H. *Coord. Chem. Rev.* **2004**, *248,* 2201−2237.

10.1021/om048987r CCC: $30.25
Publication on Web 04/13/2005

Table 1. Summary of Data Collection, Solution, and Refinement Parameters for 2a and 2b

	2a	2b
empirical formula	$[(C_5H_5)Ru(PC_6H_{12}N_3)(PC_6H_{12}N_3H)Cl][PF_6]\cdot 3H_2O$	$[(C_5H_5)Ru(PC_6H_{12}N_3H)_2Cl][PF_6]_2\cdot 2H_2O$
fw	715.87	843.82
T (K)	123(2)	100(2)
wavelength (Å)	0.71073	0.71073
cryst syst/space group	orthorhombic, *Pna*2(1)	triclinic, $P\bar{1}$
a (Å)	26.2152(19)	6.5764(9)
b (Å)	14.9540(11)	13.4764(19)
c (Å)	6.4535(5)	17.321(2)
α (deg)	90	75.545(2)
β (deg)	90	81.394(2)
γ (deg)	90	82.551(2)
volume (Å^3)	2529.9(3)	1462.9(3)
Z	4	1
D_{calc} (Mg/m^3)	1.864	1.907
absorp coeff (mm^{-1})	0.994	0.953
cryst size, mm^3	0.085 × 0.085 × 0.279	0.09 × 0.09 × 0.02
θ range for data collection (deg)	1.55 to 27.89	1.75 to 25.00
index ranges	$-33 \le h \le 22, -19 \le k \le 17, -8 \le l \le 8$	$-7 \le h \le 7, -16 \le k \le 16, -20 \le l \le 20$
reflns collected/unique	5488 [R(int) = 0.0845]	5149 [R(int) = 0.1425]
absorption corr	SADABS	SADABS
data/restraints/params	5488/1/338	5149/0/388
goodness-of-fit on F^2	0.928	0.929
final R indices [$I>2\sigma(I)$]	R1 = 0.0471, wR2 = 0.0918	R1 = 0.0669, wR2 = 0.1353
R indices (all data)	R1 = 0.0745, wR2 = 0.0984	R1 = 0.1534, wR2 = 0.1524

of metal hydrides in aqueous environments is important in gaining understanding of catalysis in aqueous media. We have recently published the synthesis and reactivity of the water-soluble ruthenium half-sandwich complex $CpRu(PTA)_2H$ (**1**)[23] implicated in the biphasic hydrogenation of benzylidene acetone.[24] Herein, we report the effect of pH on the protonation of $CpRu(PTA)_2H$ and the effect of pH, salts, and H_2 pressure on the biphasic hydrogenation of benzylidene acetone.

Experimental Section

Materials and Methods. All reagents were obtained from commercial sources, checked by NMR and GC/MS, and used as received. Solvents were distilled from standard drying agents (Na/benzophone for THF, hexanes; Mg/I_2 for MeOH) or purged with nitrogen before use. High-purity hydrogen gas was purchased from Sierra Airgas and used without further purification. $CpRu(PTA)_2H$ (**1**),[23] $CpRu(PTA)_2Cl$ (**2**),[24] and PTA[9,25] were prepared as described in the literature. Hydrogenations were conducted in a 60 mL glass Fischer-Porter bottle (Andrews Glass Co.) equipped with a magnetic stirrer, pressure gauge, and rupture disk. GC/MS analyses were obtained using a Varian CP 3800 GC (DB5 column) equipped with a Saturn 2200 MS and a CP 8400 AutoInjector. ^{1}H and ^{31}P NMR spectra were recorded on either a Varian Unity Plus 500 FT-NMR spectrometer, a GN 300 FT-NMR/Scorpio spectrometer, or a QE 300 FT-NMR/Aquarius spectrometer. Proton spectra were referenced to residual solvent relative to TMS. Phosphorus chemical shifts are relative to an external reference of 85% H_3PO_4 in D_2O with positive values downfield of the reference.

Hydrogenation Procedure. All catalytic reactions were carried out in a 60 mL Fischer-Porter bottle. In a typical run, 5 mL of a 1.1mM aqueous solution of $CpRu(PTA)_2H$, 0.0146 g (0.1 mmol) of benzylidene acetone, 3 mL of phosphate buffer, and 5 mL of diethyl ether were added to the reaction vessel in a nitrogen-filled glovebox. The vessel was then sealed, taken out of the glovebox, purged three times with H_2, and stirred under H_2 pressure (60 psi). The pressure was kept constant during the catalysis by continuously feeding from a high-pressure reservoir. All reactions were done at room temperature (25 °C), and the stirring was kept constant. At the end of the required length of time, the reactor was removed and vented, and the organic products were extracted with diethyl ether. The organic layer was analyzed by gas chromatography and ^{1}H NMR spectroscopy. The peaks were identified by comparison with authentic samples, and calculation of product concentrations was performed.

Preparation of Phosphate Buffer. Phosphate buffers of desired pH were prepared using 0.1 M solutions of NaH_2PO_4, Na_2HPO_4, Na_3PO_4, and HCl/HBF_4 in the following percent volume ratios: pH 2.1 (HCl or HBF_4)/NaH_2PO_4 (95/5); pH 3.6 HCl/NaH_2PO_4 (5/95); pH 4.7 NaH_2PO_4 (100); pH 6.5 NaH_2PO_4/Na_2HPO_4 (70/30); pH 7.0 NaH_2PO_4/Na_2HPO_4 (60/40); pH 9.8 Na_2HPO_4/Na_3PO_4 (50/50). The pH of each buffer was verified by measurement with a Fisher Accumet AR50 pH meter.

Salt Effect. The influence of salts on the catalytic hydrogenation of benzylidene acetone was investigated by adding one of the following salts to the reaction prior to catalysis: 0.120 g (1.6 mmol) of KCl, 0.176 g (1.6 mmol) of $NaBF_4$, 0.268 g (1.6 mmol) of $NaPF_6$, or 0.136 g (1.6 mmol) of $NaNO_3$. In each case 5.5×10^{-3} mmol $CpRu(PTA)_2H$, 0.0146 g (0.1 mmol) of benzylidene acetone, 3 mL of pH 4.7 buffer solution, and 5 mL of diethyl ether were added to the Fischer-Porter bottle along with the desired salt. The Fisher-Porter bottle was purged and pressurized with 60 psi H_2 and the reaction run for 6 h. The results were compared to catalytic runs done for the same time interval and composition but with no additional salt present.

Synthesis of [CpRu(PTA)(PTAH)Cl](PF$_6$) (2a). $CpRu(PTA)_2Cl$ (0.010 g, 0.038 mmol) was dissolved in 0.7 mL of H_2O and 1 equiv of HPF_6 added. The solution was layered with methanol, yielding yellow crystals overnight at room temperature. A crystal suitable for X-ray diffraction was selected and mounted under oil on a glass fiber. Crystallographic data and data collecting parameters are listed in Table 1.

Synthesis of [CpRu(PTAH)$_2$Cl](PF$_6$)$_2$ (2b). $CpRu(PTA)_2Cl$ (0.010 g, 0.038 mmol) was dissolved in 1 mL of 1.0 M aqueous HPF_6. The solution was layered with methanol, affording

(20) Ontko, A. C.; Houlis, J. F.; Schnabel, R. C.; Roddick, D. M.; Fong, T. P.; Lough, A. J.; Morris, R. H. *Organometallics* **1998**, *17*, 5467−5476.
(21) Heinekey, D. M.; Oldham, W. J., Jr. *Chem. Rev.* **1993**, *93*, 913−926.
(22) Jessop, P. G.; Morris, R. H. *Coord. Chem. Rev.* **1992**, *121,* 155−284.
(23) Frost, B. J.; Mebi, C. A. *Organometallics* **2004**, *23,* 5317−5323.
(24) Akbayeva, D. N.; Gonsalvi, L.; Oberhauser, W.; Peruzzini, M.; Vizza, F.; Brueggeller, P.; Romerosa, A.; Sava, G.; Bergamo, A. *Chem. Commun.* **2003**, 264−265.
(25) Daigle, D. J. *Inorg. Synth.* **1998**, *32*, 40−45.

yellow needle-like crystals after 24 h. The solvent was decanted off, and the resulting crystals were washed with acetone and dichloromethane. The crystals were then dried under vacuum, affording $[CpRu(PTAH)_2Cl](PF_6)_2$ in 60% yield (0.008 g). ^{31}P NMR (D_2O): (−15.6 ppm, singlet). ^1H NMR (300 MHz, D_2O): δ 4.75−4.89 (multiplet, 17H, C_5H_5, NCH_2N); 4.16−4.29 (AB spin system, $^2J_{(HAHB)}$ = 15.01 Hz, 12H, PCH_2N). Anal. Calcd for $C_{18}H_{34}N_5F_{12}P_4O_2ClRu$: C, 25.28; H, 4.01; N, 9.83. Found: C, 24.86; H, 4.25; N, 10.13. X-ray quality crystals were grown by the slow evaporation of an aqueous solution of **2** treated with HPF_6, yielding yellow crystals after standing overnight. A crystal suitable for X-ray diffraction was selected and mounted under oil on a glass fiber. Crystallographic data and data collecting parameters are listed in Table 1.

Computational Details. All calculations were run on a Beowulf cluster of 16 dual-processor computers operating under Linux. Theoretical calculations were performed using the Gaussian 03 program package employing the LANL2DZ basis set of Wadt and Hay[26,27] as implemented in Gaussian 03.[28] Density functional (DFT) calculations were carried out on all complexes using Becke's three-parameter hybrid method[29] coupled to the correlation functional of Lee, Yang, and Parr (B3LYP).[30] Frequency calculations were performed on all optimized structures in order to establish the nature of the extrema and to calculate values for ΔH and ΔG.

Results

Hydrogenation of Benzylidene Acetone. In a continuation of our previous work on the reactivity of $CpRu(PTA)_2H$ (**1**) we have explored the biphasic hydrogenation of benzylidene acetone. The title compound was synthesized as previously reported.[23] Using **1**, we have catalytically reduced benzylidene acetone in a biphasic H_2O/Et_2O solvent system at room temperature and low pressures of H_2 (10−150 psi), reaction 1. The organic product was extracted from the biphasic system with diethyl ether and analyzed by ^1H NMR spectroscopy and GC/MS. The results of catalysis, Table 2, show that reduction is selective for the C=C bond. The time dependence, pressure dependence, and pH profile of catalysis were examined and are discussed. The influence of salts on catalysis was investigated by adding KCl, $NaNO_3$, $NaBF_4$, or $NaPF_6$ to the reaction mixture.

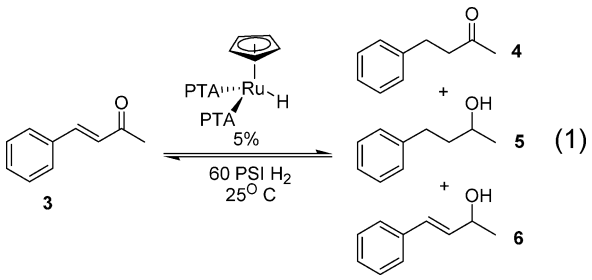

(1)

Effect of pH on Catalysis. In Table 2 the results of catalytic hydrogenation of benzylidene acetone (**3**) by **1** at various pH levels is presented. Figure 1 shows a plot of the TOF versus pH, from which it is clear that basic (pH ≥ 7) and highly acidic (pH < 3.6) pH levels result in poor catalytic performance. Compound **1** in the absence of buffer is a very poor catalyst for this reaction (Table 2, entry 1) with a conversion of only 7% after 60 h (TOF = 0.55 d^{-1}). Protonation of **1** with 1 equiv of HBF_4 produces a catalyst with a TOF of 5.28 d^{-1} (Table 2, entry 2), roughly a 10-fold increase in the catalytic efficiency of **1** alone. Catalysis at pH levels between 3.6 and 6.5 exhibited marked improvement over catalysis without a constant $[H^+]$, with pH 4.7 having the highest TOF.[31] The pH of the aqueous layer was measured before and after catalysis and remained constant. In all cases, other than entry 3, catalysis was selective for olefin hydrogenation with 4-phenylbutan-2-one (**4**) formed almost exclusively. The catalytic mixture buffered at pH 2.1 (NaH_2PO_4/HCl), Table 2, entry 3, was found to be poor, with only 7% conversion after 60 h. Interestingly, the selectivity changed yielding mostly 4-phenylbut-3-en-2-ol **6** (77.5%) along with some 4-phenylbutan-2-one **4** (22.5%). The low yields (7%) make it difficult to draw

Table 2. Effect of pH on the Hydrogenation of Benzylidene Acetone with 1

entry[a]	buffer (pH)	% conversion	TOF (d^{-1})	% **4**[b]	% **5**[b]	% **6**[b]
1	–	7	0.55	90	5	5
2[c]	–	66	5.28	92	7	<1
3	2.1[d]	7	0.55	22.5	<1	77.5
4	2.1[e]	46	3.6	>99	<1	<1
5	3.6	90	7.2[f]	>99	<1	<1
6	4.7	97	19.4[f,g]	>99	<1	<1
7	5.9	87	6.96[f]	99	1	0
8	6.5	>99	7.92[f]	>99	<1	<1
9	7.0	58	4.56	>99	<1	<1
10	9.8	11	0.89	97	3	<1

[a] $CpRu(PTA)_2H$ (5 mol %), substrate = 14.2 mg, 3 mL of 0.1 M phosphate buffer, 60 h, 25 °C. [b] Determined by GC/MS and NMR spectroscopy. [c] $CpRu(PTA)(PTAH)H]^+$ added as catalyst. [d] Buffer: HCl/NaH_2PO_4. [e] Buffer: HBF_4/NaH_2PO_4. [f] For pH 3.6−6.5 TOF determined at high conversion and may be considered a lower limit. [g] TOF and % conversion calculated after 24 h.

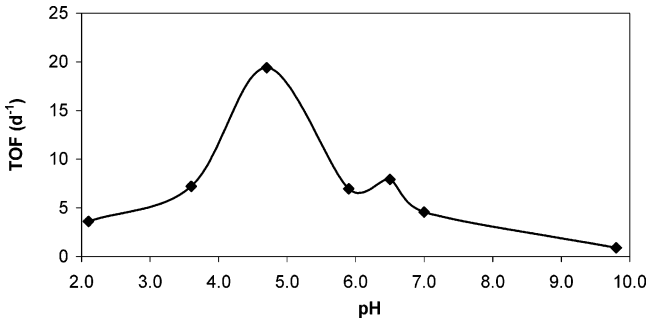

Figure 1. Plot of TOF vs pH for the hydrogenation of benzylidene acetone with **1**.[31]

(26) Wadt, W. R.; Hay, P. J. *J. Chem. Phys.* **1985**, *82*, 284−98.
(27) Hay, P. J.; Wadt, W. R. *J. Chem. Phys.* **1985**, *82*, 270−83.
(28) M. J. Frisch; G. W. Trucks; H. B. Schlegel; G. E. Scuseria; M. A. Robb; J. R. Cheeseman; J. A. Montgomery, Jr.; T. Vreven; K. N. Kudin; J. C. Burant; J. M. Millam; S. S. Iyengar; J. Tomasi; V. Barone; B. Mennucci; M. Cossi; G. Scalmani; N. Rega; G. A. Petersson; H. Nakatsuji; M. Hada; M. Ehara; K. Toyota; R. Fukuda; J. Hasegawa; M. Ishida; T. Nakajima; Y. Honda; O. Kitao; H. Nakai; M. Klene; X. Li; J. E. Knox; H. P. Hratchian; J. B. Cross; C. Adamo; J. Jaramillo; R. Gomperts; R. E. Stratmann; O. Yazyev; A. J. Austin; R. Cammi; C. Pomelli; J. W. Ochterski; P. Y. Ayala; K. Morokuma; G. A. Voth; P. Salvador; J. J. Dannenberg; V. G. Zakrzewski; S. Dapprich; A. D. Daniels; M. C. Strain; O. Farkas; D. K. Malick; A. D. Rabuck; K. Raghavachari; J. B. Foresman; J. V. Ortiz; Q. Cui; A. G. Baboul; S. Clifford; J. Cioslowski; B. B. Stefanov; G. Liu; A. Liashenko; P. Piskorz; I. Komaromi; R. L. Martin; D. J. Fox; T. Keith; M. A. Al-Laham; C. Y. Peng; A. Nanayakkara; M. Challacombe; P. M. W. Gill; B. Johnson; W. Chen; M. W. Wong; C. Gonzalez; J. A. Pople *Gaussian 03, Revision B.02*; Gaussian, Inc.: Pittsburgh, PA, 2003.
(29) Becke, A. D. *Phys. Rev. A* **1988**, *38*, 3098−100.
(30) Lee, C.; Yang, W.; Parr, R. G. *Phys. Rev. B* **1988**, *37*, 785.
(31) At this stage it is unclear what the reproducible double maximum in Figure 1 means. A change in mechanism is a possibility. At pH 6.5 only **1c** is present; however, at pH 5.9 both **1c** and **1b** are present in solution. We are currently exploring this phenomenon in more detail.

any conclusions from this result. Repeating the catalysis at pH 2.1 with buffer prepared with HBF_4 in place of HCl (Table 2, entry 4) yielded results consistent with that of other catalytic runs. The effect of Cl^- and BF_4^- anions will be discussed later in this report.

In the hydrogenation of **3** by **1** a small amount of styrene was detected by GC/MS among the other products, presumably due to decarbonylation of **3** as observed by Hernandez and Kalck for aldehydes.[32] It should be noted that at pH 4.7 we have been unable to hydrogenate styrene, and benzaldehyde was reduced to benzyl alcohol with only modest results under the conditions described (23% conversion, TOF = 2.3 d^{-1}). The hydrogenation of *trans*-chalcone (1,3-diphenylpropane-1-one) was carried out at pH 7.0 and 4.7, 60 psi H_2, 5% **1**, 25 °C. At pH 7.0 no product formation was observed over the course of 6 h; however, at pH 4.7 90% conversation of the α,β-unsaturated ketone to the saturated ketone was observed.

In comparison $CpRu(PTA)_2Cl$ (**2**) was reported to reduce **3** with modest selectivity, yielding **4**, **5**, and **6** in a ratio of 25:7:1 in an unbuffered H_2O/octane medium at 130 °C, 450 psi H_2 over 21 h (TOF = 22.8 d^{-1}).[24] Peruzzini et al. have recently reported the hydrogenation of **3** with $[(C_5H_4CH_2CH_2NEt_2)Ru(PTA)_2CH_3CN]^+$ and $[CpRu(PTA)_2(CH_3CN)]^+$, showing modest yields (~20 and 48%, respectively) with high selectivity for **4** under similar conditions, 450 psi H_2, 80 °C.[33] In the biphasic hydrogenation of benzylidene acetone by [*cis*-$[Ru(6,6'\text{-}Cl_2bpy)_2(OH_2)_2](CF_3SO_3)_2$ in water/toluene Lau and Cheng reported that the carbon−carbon double bonds were preferentially reduced, giving the saturated ketone as the predominant product in good conversion, 86%.[34] $[Ru(H)_2(TPPTS)_4]$ formed in situ under basic conditions has been shown to reduce unsaturated ketones to saturated ketones.[32]

Protonation of $CpRu(PTA)_2X$ (X = H, Cl). On the basis of the data above, it is clear that pH plays a role in catalysis, presumably due to protonation of **1**. For many M−H compounds the hydride is the kinetic site of protonation, and the dihydride complex originates from rearrangement of $Ru(\eta^2\text{-}H_2)^+$.[20−22,35−37] Compounds such as **1** may also be protonated at a ligand nitrogen, much like the system reported by Chaudret.[38] We can envision four possibilities for the site of protonation of **1**: protonation of the hydride to yield the dihydrogen species, $[CpRu(PTA)_2(H_2)]^+$ (**1a**); protonation of the metal to afford the dihydride complex, $[CpRu(PTA)_2(H)_2]^+$ (**1b**); protonation of a PTA nitrogen yielding the ammonium compounds $[CpRu(PTA)(PTAH)H]^+$ (**1c**) or $[CpRu(PTAH)_2H]^{2+}$ (**1d**); protonation of the Cp ligand yielding $[(\eta^4\text{-}C_5H_6)Ru(PTA)_2H]^+$ (**1e**). Figure 2, depicts each of the four possibilities for monoprotonation along with the DFT calculated relative energies for each. It

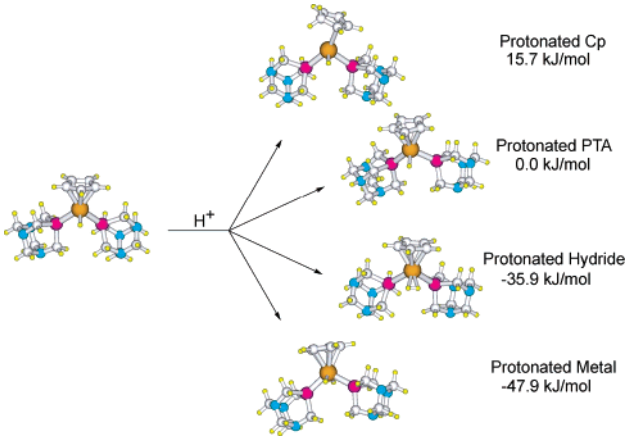

Figure 2. DFT-calculated relative energies of the various protonated species of $CpRu(PTA)_2H$.

is important to note that all four of these structures are minima on the potential energy surface, and as such they have zero imaginary frequencies. DFT calculations suggest that the most stable isomer is the dihydride, closely followed by the dihydrogen complex. The protonated Cp complex is found to be highest in energy and will not be discussed further. It seems reasonable that for compounds such as **1** the kinetic site of protonation is one of the PTA nitrogens, while the thermodynamic site of protonation may in fact be the metal.

Protonation of **1** with 1 equiv of HBF_4 results in a single compound we have tentatively assigned as $[CpRu(PTA)(PTAH)H]^+$ based on the ^{31}P NMR chemical shift of −11.5 ppm. Addition of excess HBF_4 to **1** results in a ^{31}P NMR resonance at −7.3 ppm, which we have assigned as $[CpRu(PTAH)_2H]^{2+}$, *vide infra*. $CpRu(PTA)_2H$ is not protonated by 2,6-lutidinium, and conversely, the protonated complex $[CpRu(PTA)(PTAH)H]^+$ is completely deprotonated by 2,6-lutidine, indicating the pK_a must be less than 6.5 (the pK_a of 2,6-lutidinium). On the basis of literature precedent, we would expect $Ru(H_2)^+$ or $Ru(H)_2^+$ to have pK_a values between 9 and 13 in water.[39] For comparison, the pK_a of $PTAH^+$ is 5.7, and the few reported pK_a values of metal-coordinated $PTAH^+$ complexes are between 4.69 and 2.12.[40]

Similarly, $CpRu(PTA)_2Cl$ (**2**) may be protonated with excess HPF_6, resulting in a ^{31}P NMR shift from −25.6 for **2** to −15.6 ppm for $[CpRu(PTAH)_2Cl]^{2+}$ (**2b**). Similar to **1** complex **2** cannot be protonated by [2,6-lutidinium]-(BF_4), and the protonated complex **2b** is completely deprotonated by 2,6-lutidine, affording **2**, indicating protonation of the PTA ligand. Slow evaporation of an aqueous solution of **2** and excess HPF_6 yielded yellow X-ray quality crystals of **2b** overnight. Treatment of an aqueous solution of $CpRu(PTA)_2Cl$ with 1 equiv of HPF_6 and layering the solution with methanol afforded yellow needle crystals of $[CpRu(PTA)(PTAH)Cl](PF_6)$ (**2a**).

Structure of $[CpRu(PTA)(PTAH)Cl](PF_6)$ (2a). The solid-state structure of complex **2a** was determined by X-ray crystallography. A thermal ellipsoid view of **2a** is depicted in Figure 3, along with the atomic numbering scheme and selected bond distances and

(32) Hernandez, M.; Kalck, P. *J. Mol. Catal. A: Chem.* **1997**, *116*, 131−146.
(33) Bolano, S.; Gonsalvi, L.; Zanobini, F.; Vizza, F.; Bertolasi, V.; Romerosa, A.; Peruzzini, M. *J. Mol. Catal. A* **2004**, *224*, 61−70.
(34) Lau, C.-P.; Cheng, L. *J. Mol. Catal.* **1993**, *84*, 39−50.
(35) Chinn, M. S.; Heinekey, D. M. *J. Am. Chem. Soc.* **1990**, *112*, 5166−5175.
(36) Bullock, R. M.; Song, J.-S.; Szalda, D. J. *Organometallics* **1996**, *15*, 2504−2516.
(37) Papish, E. T.; Rix, F. C.; Spetseris, N.; Norton, J. R.; Williams, R. D. *J. Am. Chem. Soc.* **2000**, *122*, 12235−12242.
(38) Ayllon, J. A.; Sayers, S. F.; Sabo-Etienne, S.; Donnadieu, B.; Chaudret, B.; Clot, E. *Organometallics* **1999**, *18*, 3981−3990.
(39) Kristjansdottir, S. S.; Norton, J. R. Acidity of Hydrido Transition Metal Complexes in Solution. In *Transition Metal Hydrides*; Dedieu, A., Ed.; VCH: New York, 1992; pp 309−359.
(40) Darensbourg, D. J.; Robertson, J. B.; Larkins, D. L.; Reibenspies, J. H. *Inorg. Chem.* **1999**, *38*, 2473−2481.

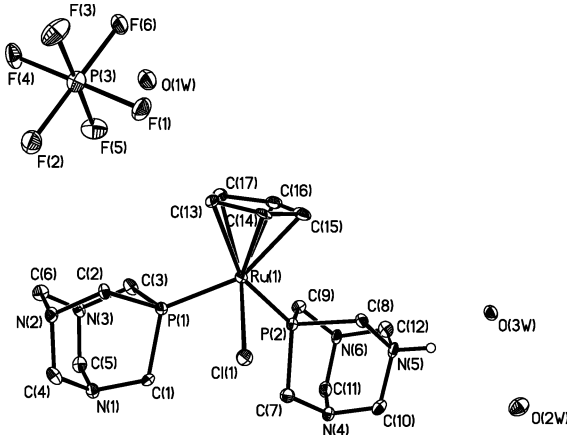

Figure 3. Thermal ellipsoid representation of [CpRu(PTA)(PTAH)Cl](PF$_6$)·3H$_2$O including the atomic numbering scheme. Hydrogen atoms have been omitted for clarity. Thermal ellipsoids are drawn at 50% probability. Selected bond lengths (Å) and angles (deg): Ru(1)−P(1) = 2.2656(17), Ru(1)−P(2) = 2.2668(16), Ru(1)−Cl(1) = 2.4683(14), Ru(1)−Cp$_{centroid}$ = 1.852, N(5)−C(10) = 1.531(7); P(1)−Ru(1)−P(2) = 98.81(5), P(1)−Ru(1)−Cl(1) = 86.53(5), P(2)−Ru(1)−Cl(1) = 87.13(5).

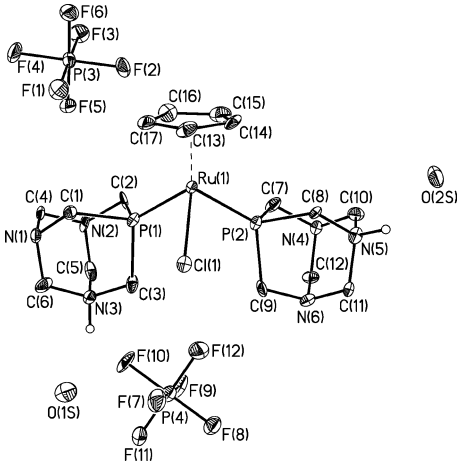

Figure 4. Thermal ellipsoid representation of [CpRu(PTAH)$_2$Cl](PF$_6$)$_2$·2H$_2$O including the atomic numbering scheme. Hydrogen atoms have been omitted for clarity. Thermal ellipsoids are drawn at 50% probability. Selected bond lengths (Å) and angles (deg): Ru(1)−P(1) = 2.254(3), Ru(1)−P(2) = 2.257(3), Ru(1)−Cl(1) = 2.455(2), Ru(1)−Cp$_{centroid}$ = 1.855, N(5)−C(10) = 1.528(11); N(3)−C(5) = 1.517(12); P(1)−Ru(1)−P(2) = 99.05(10), P(1)−Ru(1)−Cl(1) = 85.86(9), P(2)−Ru(1)−Cl(1) = 86.80(9).

bond angles. The piano stool complex **2a** consists of a cyclopentadiene ligand (Cp) bound to a ruthenium with two PTA ligands and the chloride; a PF_6^- is present to balance the charge along with three cocrystallized water molecules. The PTA ligands of **2a** are bound, as expected, through phosphorus, and are tilted away from the chloride ligand. The angle between the plane defined by the Cp ligand and the plane defined by Ru(1), P(1), and P(2) (Cp-MP$_2$) in **2a** is 55.5°, compared with 55.3° for the nonprotonated derivative recently reported by us.[23] The (N)C−N distances of one PTA ligand are found to be ∼1.47 Å, consistent with a nonprotonated PTA nitrogen.[13] The second PTA ligand has two (N)C−N distances of 1.53 Å, consistent with a protonated PTA nitrogen.

Three equivalents of water cocrystallize with **2a** in a layered structure with alternating rows of CpRu(PTA)(PTAH)$^+$ and PF_6^-/H$_2$O. Examination of the packing diagram of **2a** reveals that the layers are held together by hydrogen bonding (see Supporting Information). The N(5)···O3W separation is observed to be 2.812 Å, clearly within standard hydrogen bonding distance. O2W is more than 4 Å from N(5), well outside of normal hydrogen-bonding distance, but is only 2.721 Å from O3W, indicative of an O2W···H···O3W hydrogen bond. The O3W water is also hydrogen bound to N(2) of an adjacent [CpRu(PTA)(PTAH)]$^+$ molecule in the packing diagram; the N(2)···O3W distance is 2.754.

Structure of [CpRu(PTAH)$_2$Cl](PF$_6$)$_2$ (2b). X-ray quality crystals of [CpRu(PTAH)$_2$Cl](PF$_6$)$_2$ were grown by slow evaporation of a aqueous solution of the complex. A thermal ellipsoid view of [CpRu(PTAH)$_2$Cl](PF$_6$)$_2$ is depicted in Figure 4, along with the atomic numbering scheme and selected bond distances and bond angles. The structure of [CpRu(PTAH)$_2$Cl](PF$_6$)$_2$ (**2b**) is very similar to that of **2a**. Important details may be found in Table 3. Both PTA ligands are protonated, as evidenced by the (N)C−N bond length and hydrogen-bonding pattern in the packing diagram. Two PF_6^- ions are present per Ru center to balance the charge. A comparison of the bond lengths and bond angles of **2**, **2a**, and **2b** is presented in Table 3. All three structures are remarkably similar, with the major difference observed being a slight decrease in the P1−Ru−Cl angle and a very slight increase in the P1−Ru−P2 angle upon protonation.

Table 3. Comparison of Selected Bond Lengths (Å) and Bond Angles (deg) of CpRu(PTA)$_2$Cl, CpRu(PTA)(PTAH)Cl]PF$_6$, and CpRu(PTAH)$_2$Cl](PF$_6$)$_2$

	2[a]	**2a**	**2b**
Ru−Cl	2.445(2)	2.468(1)	2.455(2)
Ru−P1	2.258(3)	2.266(2)	2.254(3)
Ru−P2	2.247(3)	2.267(2)	2.257(3)
Ru−Cp$_{cent}$	1.852	1.852	1.855
(N)C−N	1.460(2)[b]	1.465(7)[c]	1.448(11)[d]
(N)C−N(H)		1.531(7)[e]	1.516(12)[f]
P1−Ru−P2	96.85(5)	98.81(5)	99.05(10)
P1−Ru−Cl	91.61(7)	86.53(5)	85.86(9)
P2−Ru−Cl	86.46(7)	87.13(5)	86.80(9)
Cp−ML$_2$	55.3	55.5	54.1

[a] See ref 23. [b] Average of 12 values. [c] Average of 10 values. [d] Average of 8 values. [e] Average of 2 values. [f] Average of 4 values.

pH Dependent Speciation of CpRu(PTA)$_2$H. In an attempt to understand the role of pH on catalysis; we explored the nature of **1** under the reaction conditions to identify the active species. In separate NMR tubes, 15 mg of CpRu(PTA)$_2$H was dissolved in 0.6 mL of phosphate buffer (pH 2.1−9.8). ^{31}P NMR spectra of the samples were obtained at room temperature and at 5 °C. At room temperature the spectra were rather broad, with little or no coupling evident. Cooling the samples to 5° C revealed a great deal of useful information.

The results of the spectroscopic studies are presented in Figure 5. At pH 9.8 and 7.0 (Figure 5a and 5b) one doublet at −13.3 ppm ($^2J_{PH}$ = 33 Hz) is present in the ^{31}P NMR spectrum corresponding to **1**. Upon lowering the pH to 6.5 (Figure 5c), a small shift in the NMR resonance to −12.9 ppm (d, $^2J_{PH}$ = 33 Hz) is observed.

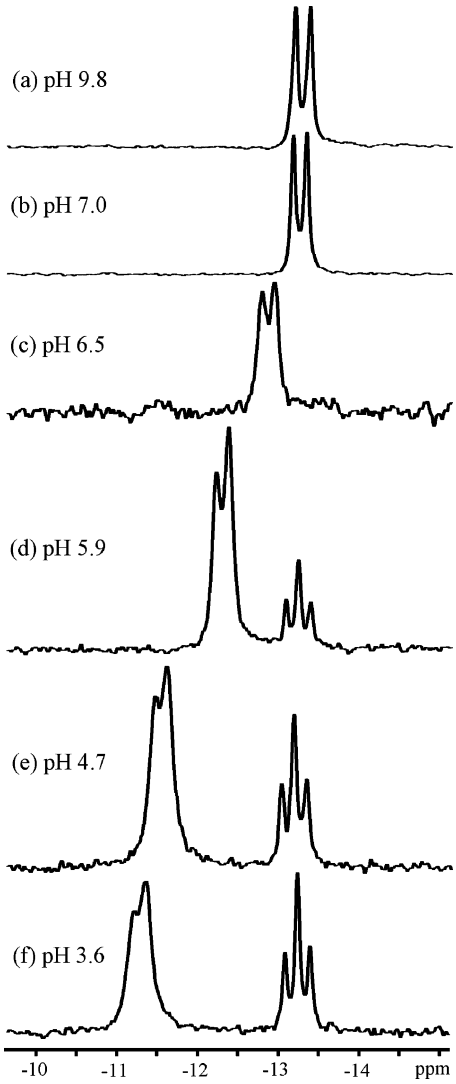

Figure 5. ^{31}P NMR spectra of **1** at various pH levels at 5 °C.

A further decrease in the pH to 5.9 (Figure 5d) resulted in two sets of resonances in the ^{31}P NMR spectrum, a doublet at −12.2 ppm ($^2J_{PH}$ = 32 Hz) and a triplet at −13.15 ppm ($^2J_{PH}$ = 32 Hz), corresponding to $[CpRu(PTA)(PTAH)H]^+$ and $[CpRu(PTA)_2(H)_2]^+$ in a ratio of 4:1. Figure 5e shows the ^{31}P NMR spectrum of **1** at pH 4.7, which indicates the presence of $[CpRu(PTA)(PTAH)H]^+$ at −11.5 ppm (d, $^2J_{PH}$ = 31 Hz) and $[CpRu(PTA)_2(H)_2]^+$ at −13.15 ppm (t,$^2J_{PH}$ = 31 Hz) in a ratio of 2.33:1. At pH 3.6 (Figure 5f) again two sets of resonances are observed in a ratio of 1.67:1, a doublet now shifted to −11.15 ppm and a triplet that remains fixed at −13.15 ppm. From these spectra it is clear that **1** is in equilibrium with **1c**. The equilibrium constant (K_{eq}) for the exchange between **1** and **1c** at 5 °C can be approximated to be 6×10^6 L/mol, based on the average value for K_{eq} calculated from the NMR chemical shifts for each pH (6.5, 5.9, and 4.7). Presumably an equilibrium also exists between **1**, **1c**, and **1b**, although this exchange is too slow to observe on the time scale of this NMR experiment. However, since the $^2J_{PH}$ coupling is observable, we can set an upper limit on exchange equal to the coupling constant ∼31 s^{-1} at 5 °C. At room temperature all the resonances are significantly broadened, indicative of exchange; however, it is unclear if this is direct exchange between **1c** and **1b** or if the exchange is between the Ru complexes and water.

Scheme 1

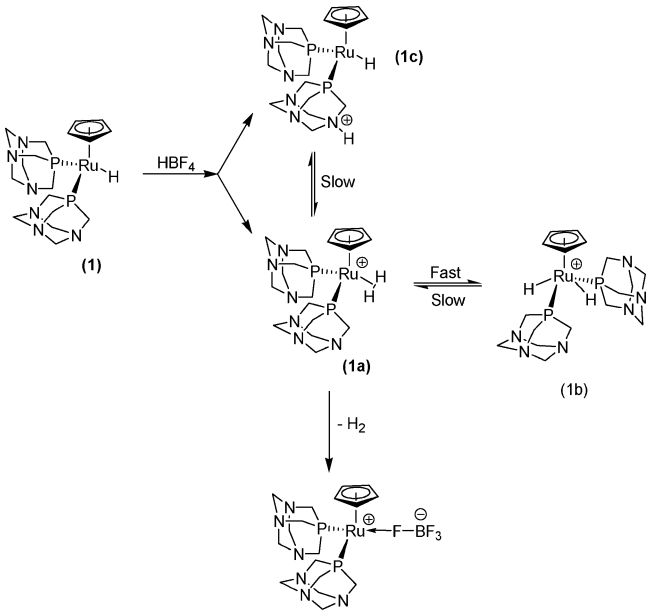

Finally, at pH 2.1, a broad resonance at −7.3 ppm in the ^{31}P NMR spectrum is observed along with the triplet slightly shifted to −12.5 ppm, **1b** (t,$^2J_{PH}$ = 31 Hz). The peak at −7.3 ppm can also be generated by treating an aqueous solution of **1** with excess HBF_4. An aqua complex, $CpRu(PTA)_2(H_2O)^+$, resulting from loss of H_2, can be excluded on the basis of the ability to regenerate **1** by addition of 2,6-lutidine to the solution, reaction 2. These results show that the species at −7.3 ppm is a protonated form of **1**, which we have assigned as the diprotonated complex $[CpRu(PTAH)_2H]^{2+}$ (**1d**), although we cannot rule out a species such as the protonated dihydride $[CpRu(PTA)(PTAH)(H)_2]^{2+}$. Scheme 1 depicts the cycle of protonation we believe to occur in this system.

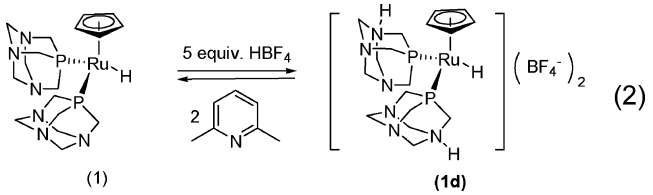

(2)

Effect of H_2 Pressure on Catalysis. The influence of H_2 pressure on catalysis was investigated at pH 4.7, room temperature, 6 h reaction time, with a pressure range of 10 to 150 psi H_2. The percent conversion increases with increasing H_2 pressure until ∼80 psi, at which time the plot of conversion versus time reaches a maximum, Figure 6. No variation in the regioselectivity of hydrogenation was observed with the change in hydrogen pressure. At H_2 pressures above 80 psi conversion falls off, suggesting that H_2 plays an inhibitory role in catalysis. It is unclear what causes this drop in activity with increasing H_2 pressure. One possibility is trapping the catalyst in a less active state, a $[CpRu(PTA)(PTAH)(\eta^2\text{-}H_2)]^{2+}$ complex for example.

Salt Effect. The influence of salts on the hydrogenation of benzylidene acetone by **1** was examined by

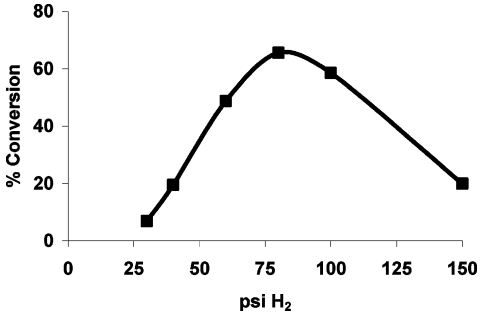

Figure 6. Pressure dependence of hydrogenation of **3**, pH 4.7, 25 °C, 5% **1**, 6 h.

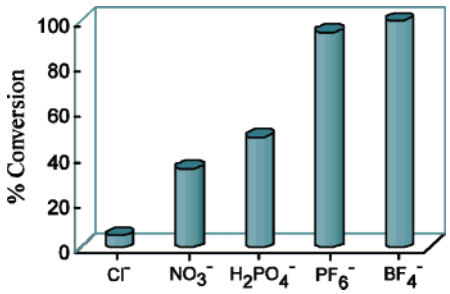

Figure 7. Salt effect for the hydrogenation of benzylidene acetone at pH 4.7: 5% **1**; H_2O/Et_2O (5 mL/5 mL); 1.6 mmol of salt (KCl, $NaNO_3$, $NaPF_6$, or $NaBF_4$); 3 mL of pH 4.7 phosphate buffer; 14.2 mg of **3**; 25 °C; 6 h.

Table 4. pH Dependence of the Hydrogenation of Benzylidene Acetone in the Presence of $NaBF_4$

entry[a]	buffer (pH)	% conversion[b] (no salt)	% conversion[b] ($NaBF_4$)	TOF (d^{-1})[c] ($NaBF_4$)
1	3.6	–	67	53.5
2	4.7	49	>99	79.2
3	5.9	7.3	65	51.8
4	7.0	0	0	0
5	9.8	0	0	0

[a] $CpRu(PTA)_2H$ (5 mol %), substrate = 14.2 mg, 0.1757 g of $NaBF_4$, 3 mL of 0.1 M phosphate buffer, 6 h, 25 °C. [b] Determined by GC/MS and NMR spectroscopy. [c] TOF and % conversion calculated after 6 h.

addition of KCl, $NaNO_3$, $NaBF_4$, or $NaPF_6$ to the catalytic mixture. The reaction mixtures were buffered at pH 4.7, put under hydrogen pressure (60 psi), and allowed to react for 6 h. The results, presented in Figure 7, clearly show a significant influence of the nature of the anion on catalytic activity. In the presence of PF_6^- or BF_4^- anions, high conversions (>95%) and improved TOF were observed. Addition of $NaNO_3$ results in conversions similar to that for the phosphate buffer alone, 35% and 49% conversion respectively, indicating that $H_2PO_4^-$ exhibits a similar salt effect as NO_3^-. Catalysis in the presence of added $NaBF_4$ exhibits the same pH dependence as catalysis in the absence of $NaBF_4$, Table 4, although the rate of reaction is much greater in the presence of BF_4^-. The reason for this increased performance is not clear, but may be attributed to stabilizing a coordinatively unsaturated intermediate generated during the reaction.

Only stoichiometric amounts of product (~5%) are obtained upon addition of KCl to the catalytic mixture. Chloride ions impede catalytic activity due to the formation of the catalytically inactive $CpRu(PTA)_2Cl$, which explains the low conversion observed at pH 2.1 (Table 2, entry 3). The formation of $CpRu(PTA)_2Cl$ under the reaction conditions was confirmed in a separate set of experiments. A solution of **1** in pH 4.7 buffer was treated with KCl. Two ^{31}P NMR signals, a doublet and a triplet corresponding to $[CpRu(PTA)(PTAH)H]^+$ and $[CpRu(PTA)_2(H)_2]^+$, respectively, were observed (*vide supra*). The kinetics of H/Cl exchange was monitored by ^{31}P NMR spectroscopy at room temperature, under pseudo-first-order conditions with respect to Cl^-. Over the course of 45 h the signals for **1b** and **1c** disappear, accompanied by a color change from pale yellow to orange and the appearance of a peak at −25.6 ppm in the ^{31}P NMR spectrum corresponding to $CpRu(PTA)_2Cl$ (**2**).[23,24] The rate constant for the formation of **2** (k_{Cl}) was found to be 7.2×10^{-6} s^{-1}. The rate constants for the disappearance of **1b** or **1c** were found to be 3.8×10^{-6} s^{-1}, approximately half that of k_{Cl}, supporting our assertion that **1b** and **1c** are in equilibrium. Under the catalytic conditions **2** is formed much more rapidly due to the formation of an open coordination site during the reaction. No formation of **2** was observed over the course of six weeks upon treatment of an aqueous solution of **1**, at pH 7.5, with KCl (Scheme 2).

Scheme 2

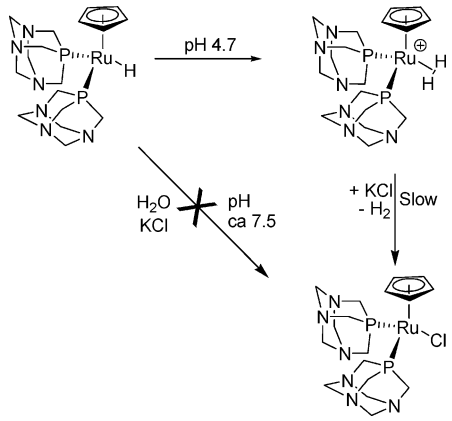

Discussion

Speciation studies on $CpRu(PTA)_2H$ at various pH levels have allowed for some insight into the mechanism of hydrogenation: identification of active species and specifically the pH dependent nature of catalysis as depicted in Table 2. At pH levels between 3.6 and 6.5 a high concentration of **1c** is observed and catalysis occurs readily. Above pH > 7.0, **1** is present in solution with moderate to poor catalytic activities; at pH 7.0 the TOF is 4.56 d^{-1}, while at pH 9.8 the TOF is an abysmal 0.89 d^{-1}. At very low pH levels, i.e., pH 2.1, the TOF is also poor, between 0.55 and 3.6 d^{-1} for buffers containing Cl^- or BF_4^- ions, respectively. The poor efficiency at very acidic pH levels is presumably due to either poor activation of H_2 by $[CpRu(PTAH)_2]^{3+}$ or a low hydricity of $[CpRu(PTAH)_2H]^{2+}$. On the basis of these results we propose that the active species in catalysis is **1c**, $[CpRu(PTA)(PTAH)H]^+$.

The effect of salts on the catalytic activity suggests that the catalytic cycle involves a coordinatively unsaturated species that is stabilized by the anion or water molecule. The coordinated anion or solvent is displaced by H_2 in the catalytic cycle. Strongly coordinated anions cannot be displaced by H_2; hence the catalytic perfor-

Scheme 3

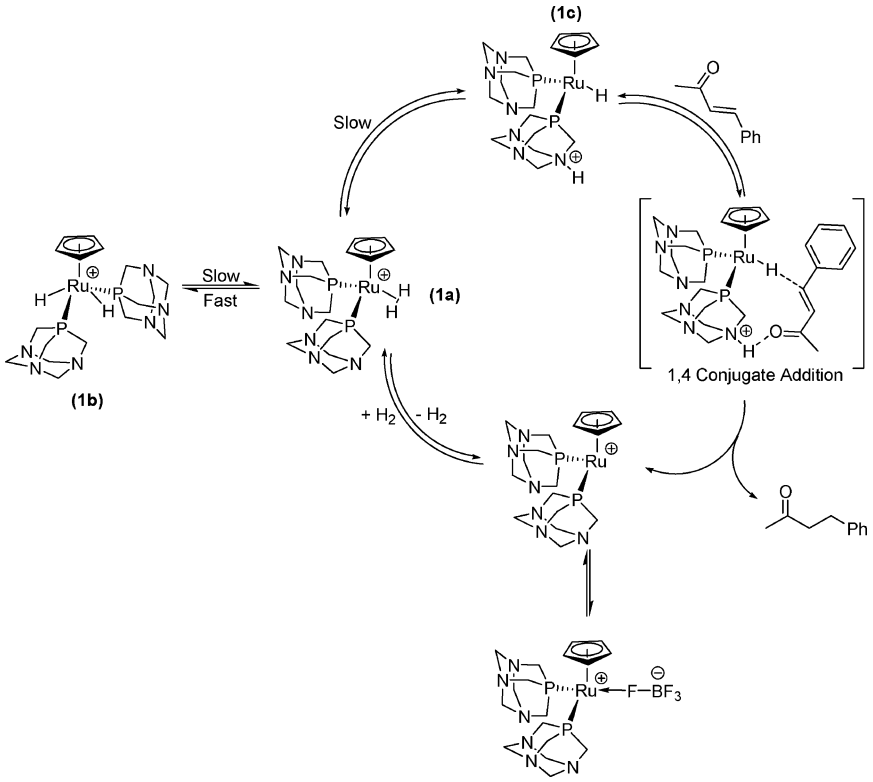

mance suffers, as is case in the presence of Cl^- ion. Weakly coordinating ions such as BF_4^- or PF_6^- enhance reactivity through a fine balance of stabilizing the coordinatively unsaturated $[CpRu(PTA)_2]^+$ from decomposition and displacement by H_2.

The active catalyst appears to be $[CpRu(PTA)(PTAH)H]^+$ (**1c**), the major species present at pH 6.5−3.6, the pH levels with the highest TOF, although we cannot rule out $[CpRu(PTA)(H)_2]^+$. **1c** allows for the addition of H_2 to the C=C bond of an α,β-unsaturated ketone through a 1,4-conjugate addition mechanism, taking advantage of Noyori's "N−H" effect.[19] In this catalytic cycle, Scheme 3, we propose a transition state in which the N−H bond in **1c** hydrogen bonds to the ketone, activating the olefin for hydride transfer from the Ru−H, a classic 1,4-conjugate addition. Hydride transfer is followed by proton transfer from either the protonated PTA or the solvent (water). The fact that the PTA nitrogen can be protonated facilitates this mechanism, which has been described as an ionic hydrogenation, involving addition of H_2 as H^+ (from a metal dihydrogen/dihydride complex, external acid, or a ligand bound proton) and H^- (from a transition metal hydride) to an unsaturated compound.[41] Ionic hydrogenations do not involve formal insertion into the M−H bond and therefore do not require an open coordination site for insertion into the M−H bond. The coordinatively unsaturated $[CpRu(PTA)_2]^+$ can then undergo H_2 addition to give a Ru-dihydrogen complex, **1a**, which undergoes rearrangement to form either **1b** or **1c**.

Conclusions

We have presented here details of the pH-dependent activity of $CpRu(PTA)_2H$ on the hydrogenation of unsaturated ketones. The active catalyst is proposed to be the cationic species $[CpRu(PTA)(PTAH)H]^+$, resulting from protonation of PTA. The hydrogenation of benzylidene acetone is reported to be highly selective (>99%) toward the reduction of C=C bonds at pH ≤ 7.0. Attempts to alter the selectivity toward the more desired unsaturated alcohols by changing the pH, hydrogen pressure, ionic strength, and nature of the anion present proved to be ineffective. We have spectroscopically identified three protonated complexes derived from **1**: $[CpRu(PTA)_2(H)_2]^+$, $[CpRu(PTA)(PTAH)H]^+$, and $[CpRu(PTAH)_2H]^{2+}$. The distribution of these complexes is influenced by changes in pH, which in turn manifests itself in changes in the reaction rates. The presence of chloride ions impedes catalytic activity due to the formation of the catalytically inactive $CpRu(PTA)_2Cl$. However, anions such as BF_4^- and PF_6^- enhance the rate of hydrogenation. We propose that the reaction occurs via an ionic hydrogenation mechanism, and specifically through a 1,4-conjugate addition utilizing the protonated PTA as a hydrogen bond donor activating the olefin for nucleophilic attack.

Acknowledgment. This research was supported by the University of Nevada (JFRG). We thank Cytec for the generous gift of $P(CH_2OH)_4Cl$. Financial support from the National Science Foundation (CHE-0226402) is acknowledged for funding for the X-ray diffractometer.

Supporting Information Available: Complete details of the crystallographic study (PDF and CIF), plot of conversion vs time in the hydrogenation of **3**, and table of percent conversion as a function of salt for the hydrogenation. This material is available free of charge via the Internet at http://pubs.acs.org.

(41) Bullock, R. M. *Chem. Eur. J.* **2004**, *10,* 2366−2374.

OM048987R